

Electrochemical behavior of self-ordered titania nanotubes prepared by anodization as a promising material for biomedical applications.

Al-Swayih A. A.

Dep. of Chemistry, College of Science, Princess Nora Bint Abdul Rahman University, Saudi Arabia

E-mail: aswayih@yahoo.com

Abstract: Nanotube oxide layer formation was achieved from biomedical titanium using anodization technique in 1 M H₃PO₄ + 0.8 wt.% NaF. The effect of anodization time and potential was studied. The nanotubes surface was characterized using SEM, and the electrochemical behavior was investigated employing open circuit potential, electrochemical impedance spectroscopy and potentiodynamic polarization measurements in Hank's solution. The results indicate that there is a minimum potential required for the formation of titanium nanotubes. The oxide nanotubes length and diameter vary with anodization potential, leading to a different electrochemical behavior in Hank's solution. The titanium oxide nanotube formed at 20 V has the lower I_{corr} and higher E_{corr}, which indicates the best stability in Hank's solution. On the other hand, the duration of anodization process up to 2 hour doesn't have a pronounced effect on the surface morphology, but it can change the stability of titanium oxide nanotubes, which was indicated by the electrochemical parameters. This effect can be attributed to the rate of the dissolution reaction occurring at the titanium oxide nanotube surface in Hank's solution.

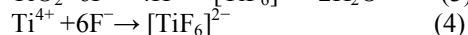
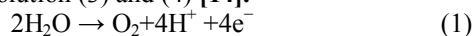
[A. A. Al-Swayih. **Electrochemical behavior of self-ordered titania nanotubes prepared by anodization: A promising material for biomedical applications.** *J Am Sci* 2014;10(10):165-173]. (ISSN: 1545-1003). <http://www.jofamericanscience.org>. 25

Key words: Biomaterials – nanostructures - electrochemical properties - corrosion test

1. Introduction

Titanium dioxide (TiO₂) nanotube arrays are of great interest due to its application in solar cells [1], gas sensors [2], photo-catalysis [3], photo-electrochemical hydrogen generation [4], orthopedic implants [5], etc. Titania nanotubes have been prepared by a variety of techniques including sol-gel method [6], electrophoretic deposition [7], hydrothermal [8,9] and anodization [10,11]. Amongst the various methods of processing titania nanotubes, anodization of metallic titanium resulting in vertically aligned TiO₂ nanotubular arrays is a simple and cost-effective electrochemical process. A major advantage of anodization is the feasibility to tune the size and shape of nanotubular arrays to the desired dimensions, meeting the demands of specific applications by means of controlled anodic oxidation of the metal substrate. Gong et al. first reported the formation of uniform titania nanotube arrays by anodization of titanium in hydrofluoric acid as electrolyte [12].

The formation of nanotubes in fluoride containing electrolytes is the result of the interplay between three simultaneously occurring processes-field assisted oxidation of Ti metal to form titanium dioxide, field assisted dissolution of Ti metal to form titanium dioxide and chemical dissolution of Ti and TiO₂ due to etching by fluoride ions [13]. The following equations represent the oxide layer formation (1) and (2) and dissolution (3) and (4) [14].



The TiO₂ nanotube films have been extensively explored as adhesion and growth support platforms for bone and stem cells, for the prevention of bacterial adhesion, drug delivery and enhancing blood clotting for control of haemorrhage [15,16]. Favourable bone cell growth, cell differentiation, and apatite-forming abilities were demonstrated on implants with nanotubular titania surfaces demonstrating its promise for bone implants [17,18]. Recently development in stem cell research demonstrated that titania nanotubes are able to differentiation of mesenchymal stem cells into specific cells (osteoblasts) [19]. Furthermore, the outstanding photocatalytic properties of the nanotube surface were applied to photo-induced killing of cancer cells which suggests a possible application of nanotubes for an anticancer treatment [20].

These nanotube structures are produced in a controlled manner by optimizing parameters including anodization potential, electrolyte composition and properties such as pH, conductivity, viscosity, as well as anodization time and temperature [21-23]. It should be possible to control the nanotube size and morphology for biomedical implant surface by controlling the conditions of anodization process [24]. The purpose of this research work is to study the effect of anodization potential and time on the electrochemical properties of resulted titanium nanotube in Hank's solution for biomedical applications.

2. Materials and methods

2.1. Titanium oxide nanotube layer formation

Ti foils with an area of 20 mm x 30 mm and thickness of 0.25 mm (99.5% metal basis, Alfa Aesar) were used as starting material in order to obtain the titanium oxide (TiO₂) nanotube arrays. A preliminary treatment was performed by degreasing the titanium foils using sonication in acetone, in isopropanol, and then in methanol. The foils were subsequently rinsed with deionized water and dried in a nitrogen stream. TiO₂ nanotube arrays were formed by anodization in 1.0 M H₃PO₄ + 0.8 wt.%NaF. A potentiostatic anodization was conducted at different voltages viz. 10, 20, 30 and 40 V. Initially anodization was done by ramping up to the specific end potential with a ramping speed of 1 V s⁻¹ and holding it for 30 min at room temperature. Anodization was also performed as a function of time at constant voltage (20 V) at room temperature. Following the anodization, the samples were rinsed with deionized water and dried in a nitrogen stream.

2.2. Surface characterization

The surface morphology of the titanium oxide nanotube arrays was characterized using a scanning electron microscope (Jeol JSM-7600F Field-Emission Scanning Electron Microscope).

2.3. Electrochemical tests

All electrochemical measurements were performed in Hank's physiological solution, which was prepared according to an earlier report [25]. In brief, the solution was prepared using the following chemicals viz., NaCl (8.00g), KCl(0.40g), CaCl₂ (0.19g), NaHCO₃ (0.35 g), Na₂HPO₄(0.06 g), MgCl₂.6H₂O (0.19g), MgSO₄.7H₂O (0.06 g) and Glucose (1.00g). All the chemicals were dissolved in that order in 1000 mL double distilled water, the temperature was maintained at 37 °C, and the pH of the solution was 7.8.

A conventional three-electrode electrochemical cell system was used. Saturated calomel electrode (SCE) and platinum mesh were used as reference and counter electrodes, respectively. Potentials in the text refer to the SCE scale.

In the experiments, the open circuit potential (E_{OCP}) was measured for an hour. Then, electrochemical impedance spectroscopy (EIS) was recorded. The frequency ranged from 100 kHz to 10 mHz at 10 cycles per decade, with an ac amplitude of ±10 mV. The absolute impedance and phase angle were measured at each frequency. The impedance data were interpreted on the basis of equivalent electrical circuits, using the Zsim program for fitting the experimental data. In potentiodynamic polarization (PD) tests, the working electrode potential was continuously increased from -0.250 to 0.500 V relative to the E_{OCP} at a scan rate of 1 mV/s.

3. Results and Discussion

3.1. Effect of anodization voltage

3.1.1 Surface morphology

The surface morphology of Ti foils anodized at different potentials varying from 10 to 40 V for 30 min, in room temperature as shown all in Fig. 1. When the applied potential was 10 V (fig. 1(a)), formation of nanotubes was observed. The resulted nanotube had a diameter of about 31 nm, and a length of about 280 nm. Previous study was reported 10 V as the lowest required potential for the formation of nanotubes in aqueous medium containing HF as the etching agent [12]. However, another work reported that porous structures formed on the Ti surface, no distinct nanotubes when Ti anodized at 10 V in ethylene glycol containing 0.5 wt% ammonium fluoride and 2.5 wt% of water [26]. These observations indicate that there is a minimum potential required for the formation of self-organized nanotubes.

The diameter and the length of the oxide nanotubes increase when the applied potential increases to 20 V as shown in fig.1 (b), they become about 93 nm and 480 nm, respectively. The increase in tube diameter with voltage may be attributed to the enhanced chemical dissolution of TiO₂ at the pore wall. The variation of tube length with applied potential may be attributed to the increasing in the rate of chemical dissolution and oxidation, when the potential is increased, leading to an increase in nanotube growth [26]. When the anodization potential was 30 V, the current density increased with time and nanotubes well be defects on the foil. This is attributed to the enhanced rate of chemical dissolution at high potentials. It has been shown that the break down period or the time for loss of passivation decreases with increase in some factors as temperature, electrolyte concentration and the presence of fluoride ions [27]. In the present case with increase in voltage, current may increase raising the bath temperature leading to enhancement in chemical dissolution rate. Thus, when titanium anodized at 30 V, the nanotube length increases more, and the surface nanotube not well ordered, as shown in fig.1(c). If the anodization potential rise to 40 V, the increase in the nanotube length will cause a defect surface, as seen in fig.1(d).

The growth rate of the titanium oxide nanotubes for a specified set of experimental parameters is dependent on the applied voltage, in consistence to high-field oxidation theories [28-30]. From SEM images, it is seen that smooth walled nanotube arrays are obtained at 20 V.

3.1.2. Electrochemical tests

The open circuit potentials (E_{OCP}) reflect the composite results of the electrochemical reactions taking place at the electrode and solution interface. Therefore, the variation in the E_{OCP} with immersion

time can be employed to study the electrochemical processes. Fig. (2) displays the E_{OCP} of Ti nanotube samples as a function of immersion time in Hank's solution. The E_{OCP} of all samples decreases gradually towards a negative direction during the first immersion duration and it becomes constant after about 15 min. It is noted that the samples have different constant E_{OCP} value. The two samples which were anodized at 20 and 30 V have the less value of E_{OCP} , while the higher value of E_{OCP} was recorded for Ti anodized at 40 V.

This behavior may be attributed to the thickness of the oxide layer. From the SEM results, when titanium anodized at higher potential, the oxide layer will be thickening, leading to a shift of the potential in the noble direction. On the other hand, the lower E_{OCP} for nanotubes formed at 20 and 30 V, may be attributed to the effect of the diameter of the oxide nanotube. The larger pore diameter in the TiO_2 nanotube array introduces a larger effective exposed area in close proximity with the electrolyte thus enabling diffusion of corrosive ions in the electrolyte [31,32]. The diameter of the titanium oxide nanotubes formed at 10 V is smaller than that of the others, thus they have the higher E_{OCP} .

The representative polarization curves obtained from the specimens in Hank's solution are displayed in Fig. (3). The corresponding corrosion parameters are shown in Table (1). The E_{corr} of the samples was in agreement with that obtained from the open circuit potential measurements. The higher E_{corr} value for titanium oxide nanotube formed at 40 V, while the lowest for titanium oxide nanotube formed at 20 V. As seen from fig. (3) and table (1), the I_{corr} increases when the potential of anodization process increases from 10 to 30 V.

In the case of the nanotubular surface, the tubes may act as more effective channels for the electrolyte to reach the interface. The lower corrosion resistance property when titanium anodized at 20 and 30 V may be associated with the concave shaped tube bottom and the distinctly separated tube bottom/barrier oxide interface, as proposed by [33]. Also, the thickening of oxide layer when titanium anodized at 40 V will shift the I_{corr} to less value, and E_{corr} to more noble value than the other samples.

EIS is a powerful technique to study the behavior and the corrosion of metals or alloys. It can provide quantitative evaluation of the electrochemical properties of the studied system, which may be difficult to assess using conventional electrochemical measurements such as potentiostatic or potentiodynamic techniques. By appropriate interpretation of the EIS data in conjunction with an equivalent circuit (EC), detailed information on the electrochemical process at the film/solution interface can be disclosed [34].

As shown in Fig.(4); the typical EIS spectra of the four samples, which anodized at different potential. A satisfactory fit of all EIS data can be obtained by an $R_s(R_1Q_1)(R_2Q_2)$ circuit, where R_s is the solution resistance between the reference and working electrodes. Its value depends on the conductivity of the test medium and the geometry of the cell [35].

R_1 represents the charge transfer resistance of the outer nanotube layer. Q_1 is the constant phase element of the outer nanotube layer. R_2 is the resistance of the inner barrier layer, and Q_2 is corresponding to the inner barrier layer [36,37]. The schematic illustration of the oxide film as well as equivalent circuit are shown in Fig. (5). The electrochemical parameters by fitting the circuits (error of less than 10%) are presented in Table (2).

The difference in the values of the parameters can be ascribed to the morphology of the sample surface, which depends on the anodized potential. As we noted previously, when titanium anodized at 10 V the obtained nanotube has a value of R_1 and R_2 higher than that of other samples. However, as the anodization potential increase to 30 V, the values of R_1 and R_2 decrease. This EIS results are consistent with those of open circuit potential vs. immersion time, and potentiodynamic polarization measurements.

The electrochemical results suggested that the potential used in the anodization process to form titanium nanotube is an important factor, it can determine the morphology of the nanotube, and subsequent the electrochemical behavior of the sample.

3.2. Effect of anodization time

3.2.1 Surface morphology

As shown in Fig. (6); SEM images of titanium oxide nanotubes formed with different anodizing times under 20 V anodizing voltage. When the anodization time was 10 min, nanotubes were not completely formed on the surface. As shown in fig. 6 (a) there are some areas for nanotube, while the others are covered by compact oxide. The diameter of formed nanotube is about 55 nm, and its length is approximately 250 nm.

However, titanium oxide nanotubes were formed completely in the samples anodized for period more than 10 min, as shown in fig 6 (b-e). This means that there is a minimum duration required to produce nanotube surface. The sizes of the obtained nanotubes are similar, with inner diameter of 70–80 nm, and length of about 500–600 nm.

3.2.2. Electrochemical tests

As shown in fig. (7), the values of immersion potential of the titanium oxide nanotube samples are approximately the same. The E_{OCP} decreases gradually towards a negative direction during the first immersion duration and it becomes constant. The E_{OCP} at the end of the test shifts to more negative values as the anodization time increases. This may be attributed to

the increase in the rate of dissolution reaction of titanium nanotube, resulting in negative shift of the E_{OCP} .

The potentiodynamic polarization plots obtained for titanium oxide nanotube samples in Hank's solution are presented in Fig. (8) which can revealed that the nanotube layer anodized at different time has approximately the same electrochemical behavior. The electrochemical parameters obtained from polarization diagrams are presented in Table (3).

As we reported from open circuit potential, when the anodization time increases, the E_{corr} of the resulted nanotube becomes more negative. The lower I_{corr} was for titanium oxide nanotube anodized for 30 min.

Fig. (9) shows the typical EIS spectra of the titanium nanotube samples, which anodized at 20 V for different periods of time. Also, it can be seen that the diameter of the semicircle in the spectra decreases when anodization duration increases.

Table (4) presents the electrochemical parameters obtained by fitting the spectra to the equivalent circuit in fig. 5 (error of less than 10%).

When titanium anodized for 30 min, the obtained nanotube has higher values of R_1 and R_2 than that of other samples. The values of R_1 and R_2 decrease when the anodization time increases, which is consistent with the results of open circuit potential and potentiodynamic polarization measurements

These results suggest that the time of the anodization process to form titanium oxide nanotube is an important factor, that can determine the stability of the nanotube, and subsequent the electrochemical behavior of the sample. In our conditions, 30 min anodization is satisfactory.

From these experiments, it is clear that the anodization time and voltage are important parameters

for fabricating titanium oxide nanotube films using an electrochemical anodization approach. The formation of the nanotube structures during anodization results from the migration of titanium ions from the interpore areas to the oxide/solution interface. At high anodizing voltages, the electric field is strong enough to mobilize the ions and their migration leaves voids in the interpore areas, eventually separating the pores from one another, and forming discrete tubelike structures [12]. Longer anodization time leads to the formation of loosely packed arrays of titanium oxide nanotubes, which decrease the stability of the nanotube. These observations can be attributed to the different rates of dissolution and transportation of titanium ions during the formation of titanium oxide nanotubes via the above mechanism [38].

Thus, it should be possible to control the nanotube size and morphology for biomedical implant surface by controlling the potential and the time of anodization process, in addition to other factors, as chemical composition of the solution employed in anodization and the temperature.

Table 1: Electrochemical parameters obtained from potentiodynamic polarization plots for titanium nanotube prepared at different anodization potential

Anodization potential (V)	E_{corr} V	I_{corr} mA cm ⁻²
10	-0.413	8.21×10^{-5}
20	-0.472	0.85×10^{-3}
30	-0.442	6.67×10^{-3}
40	-0.285	1.25×10^{-3}

Table 2: Fitted electrochemical parameters determined from Nyquist diagrams presented in fig. 4 based on the equivalent circuit

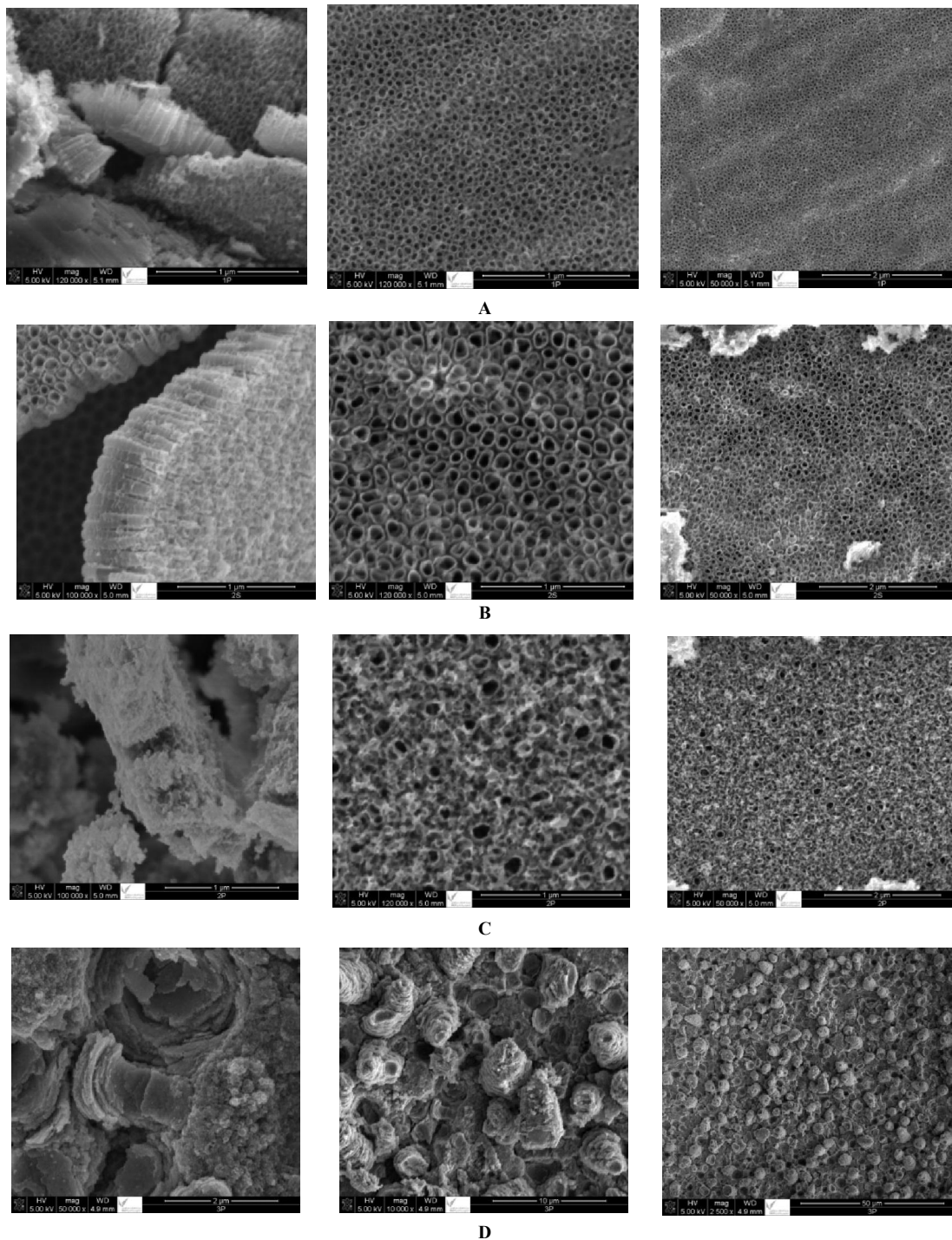
Anodization potential (V)	R_s ohm cm ²	$R_1 \times 10^3$ ohm cm ²	$Q_1 \times 10^{-4}$ F cm ⁻²	n_1	$R_2 \times 10^3$ ohm cm ²	$Q_2 \times 10^{-4}$ F cm ⁻²	n_2
10	19	30.4	0.71	0.94	71.2	0.49	0.90
20	43.1	7.95	3.06	0.94	3.68	2.11	0.91
30	92.5	1.48	5.99	0.94	0.59	5.98	0.88
40	30.8	20.5	0.70	0.96	8.53	0.93	0.91

Table 3: Electrochemical parameters obtained from potentiodynamic polarization plots for titanium nanotube prepared at different anodization time

Anodization time (min)	E_{corr} V	I_{corr} mA cm ⁻²
10	-0.506	3.36×10^{-3}
20	-0.443	2.07×10^{-3}
30	-0.472	0.85×10^{-3}
60	-0.518	2.77×10^{-3}
120	-0.564	1.50×10^{-3}

Table 4: Fitted electrochemical parameters determined from Nyquist diagrams presented in fig. 9 based on the equivalent circuits

Anodization time (min)	R_s ohm cm^2	$R_1 \times 10^3$ ohm cm^2	$Q_1 \times 10^{-4}$ F cm^{-2}	n_1	$R_2 \times 10^3$ ohm cm^2	$Q_2 \times 10^{-4}$ F cm^{-2}	n_2
10	143	2.62	5.6	0.94	1.28	3.39	0.90
20	57.6	4.61	3.31	0.94	3.43	1.67	0.88
30	43.1	7.95	3.06	0.94	3.68	2.11	0.91
60	30.3	3.11	6.81	0.96	1.01	4.84	0.91
120	38.9	1.96	0.144	0.95	1.10	5.80	0.90

**Fig. 1: The SEM images of titanium oxide nanotubes formed at different potentials : (a) at 10 V, (b) at 20 V, (c) at 30 V and (d) at 40 V**

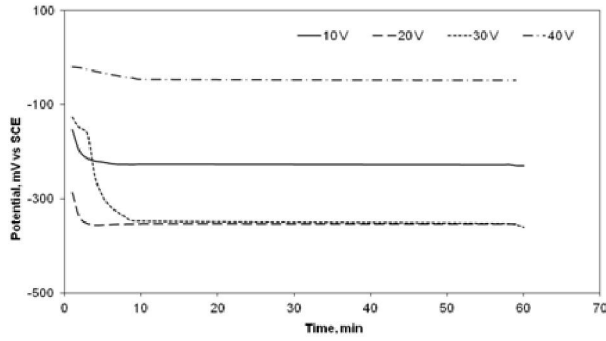


Fig. 2: The E_{OCP} of titanium oxide nanotube samples anodized for 30 min at different potentials in Hank's solution

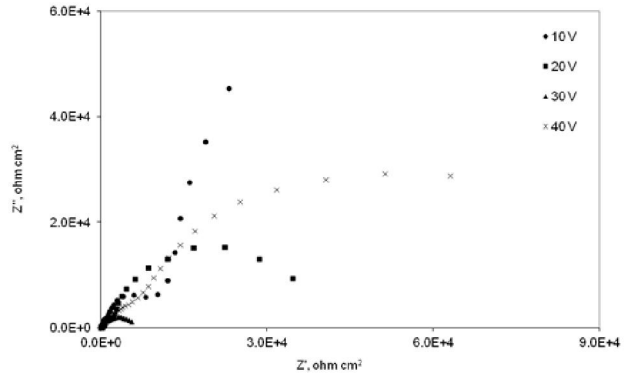


Fig.4: Nyquist diagrams of titanium oxide nanotube samples anodized for 30 min at different potentials in Hank's solution

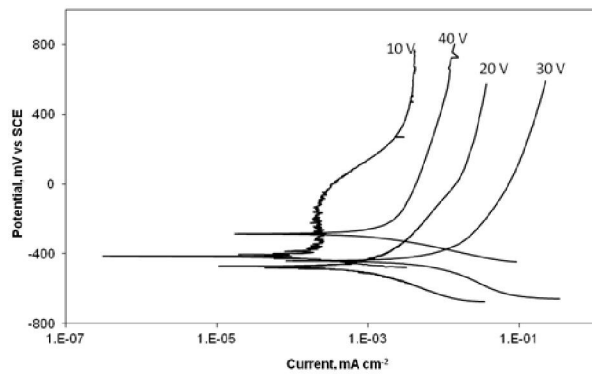


Fig. 3: Potentiodynamic polarization plots of titanium oxide nanotube samples anodized for 30 min at different potentials in Hank's solution

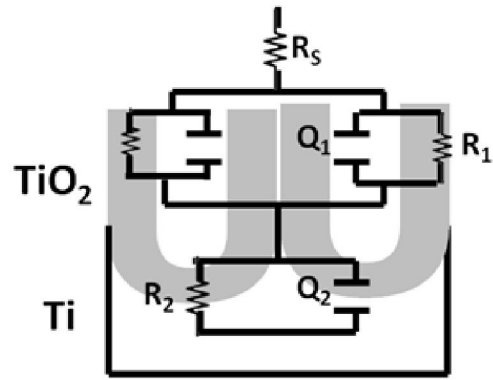
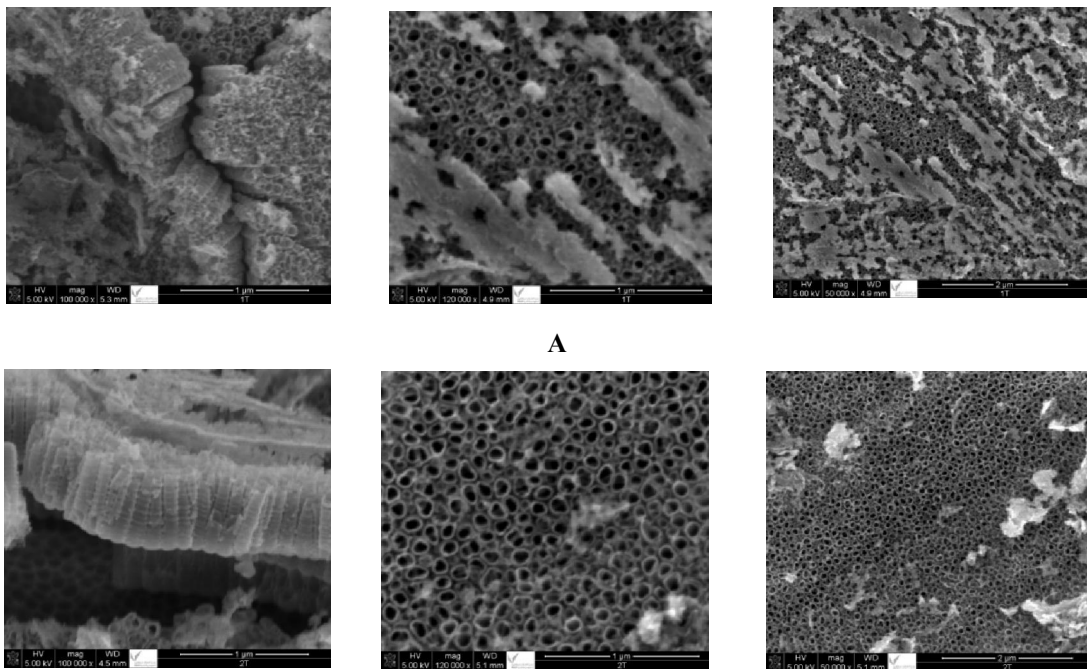


Fig. 5: Equivalent circuit used to model impedance spectra of titanium oxide nanotube



A

B

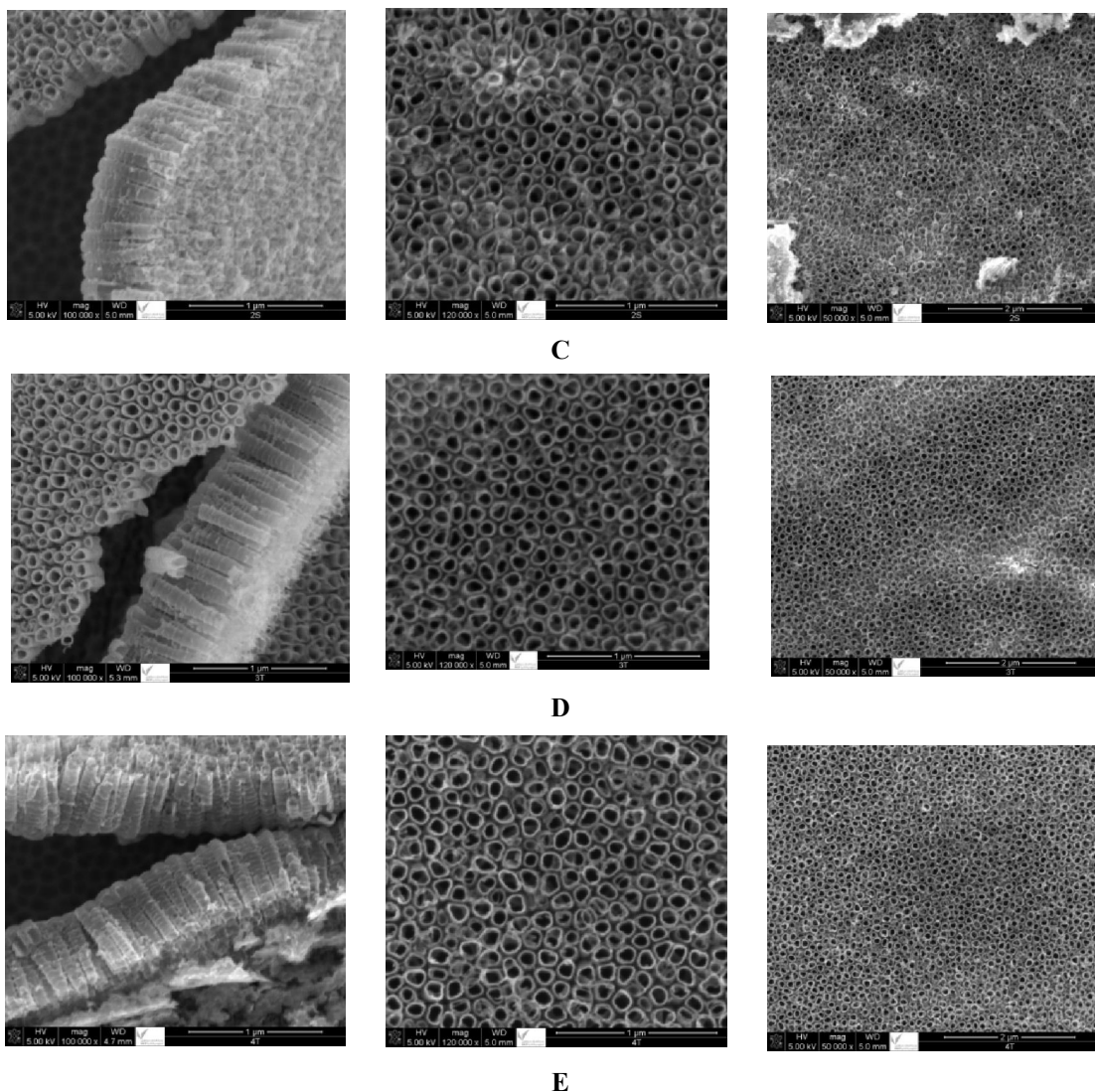


Fig. 6: The SEM images of titanium oxide nanotubes formed at 20 V for different times: (a) 10 min, (b) 20 min, (c) 30 min, (d) 60 min and (e) 120 min.

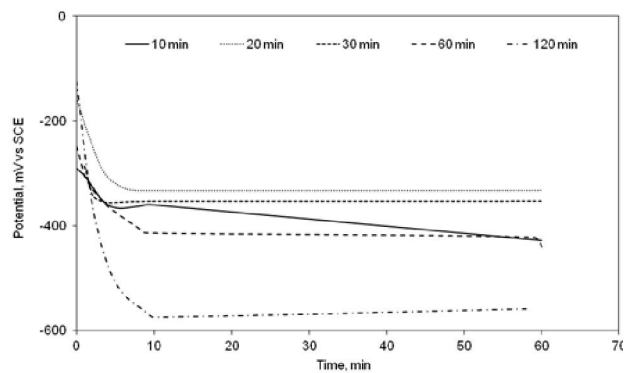


Fig. 7: The E_{OCP} of titanium oxide nanotube samples anodized at 20 V for different times in Hank's solution.

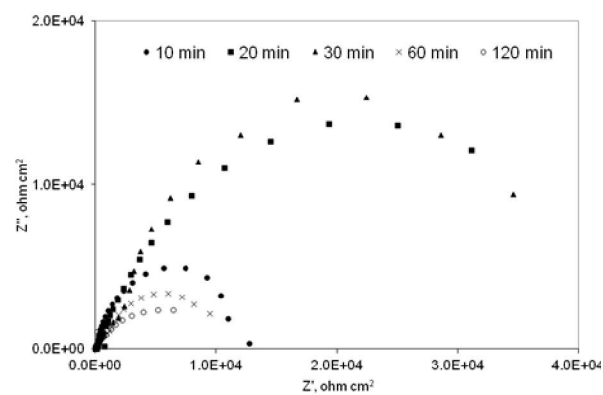


Fig. 8: Potentiodynamic polarization plots of titanium oxide nanotube samples anodized at 20 V for different times in Hank's solution (the numbers near the curve indicate the anodization time in minutes).

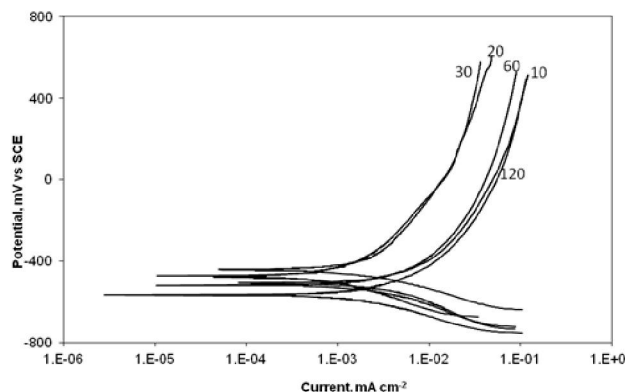


Fig.9: Nyquist diagrams of titanium oxide nanotube samples anodized at 20 V for different times in Hank's solution

4. Conclusions

Titanium nanotube oxide layers were developed on Ti using the anodization in electrolyte containing 1 M H_3PO_4 and 0.8 wt.% NaF at room temperature at different potential and for different periods of time. There is a minimum potential required for the formation of self-organized nanotubes. The nanotubes length and diameter vary with anodization potential. The differences in the surface morphology of nanotubes anodized at different potential, can effect on its behavior in Hank's solution. The titanium nanotube formed at 20 V has the best stability in Hank's solution. On the other hand, the duration of anodization process doesn't have a pronounced effect on the surface morphology, but it can effect on the stability of titanium nanotube. Thus, it should be possible to control the nanotube size and morphology for biomedical implant surface by controlling the variables of the anodization process.

Acknowledgment

The author gratefully acknowledge the financial aid from the Deanery of Scientific Research of the University of Princess Norah bint Abdulrahman, Riyadh, Kingdom of Saudi Arabia to the Research Project number 026-K-32.

References:

- Paulose M.; H.E. Prakasam; O.K. Varghese; L. Peng; K.C. Popat; G.K. Mor; T.A. Desai and C.A. Grimes (2007): TiO_2 Nanotube Arrays of 1000 μm Length by Anodization of Titanium Foil: Phenol Red Diffusion, *J. Phys. Chem. C*, 111: 14992
- Varghese O.K.; S. Yang; S. Kendig; M. Paulose; K. Zeng; C. Palmer; K.G. Ong and C.A. Grimes (2006): A transcutaneous hydrogen sensor: from design to application, *Sens. Lett.* 4: 120.
- Raja K.S.; V.K. Mahajan and M. Misra (2006): Determination of photo conversion efficiency of nanotubular titanium oxide photo-electrochemical cell for solar hydrogen generation, *J. Power Sources* 159: 1258.
- Webster T.J.; C. Ergun; R.H. Doremus; R.W. Siegel and R. Bizios (2000): Enhanced functions of osteoblasts on nanophase ceramics, *Biomaterials* 21: 1803.
- Das K.; S. Bose and A. Bandyopadhyay (2007): Surface modifications and cell-materials interactions with anodized Ti, *Acta Biomater.* 3: 573.
- Miao Z.; D. Xu; J. Ouyang; G. Guo; X. Zhao and Y. Tang (2002): Electrochemically Induced Sol-Gel Preparation of Single-Crystalline TiO_2 Nanowires, *NanoLett.* 2: 717.
- Li G.; Z. Liu; Z. Zhang and X. Yan (2009): Preparation of Titania Nanotube Arrays by the Hydrothermal Method, *Chin. J. Catal.* 30: 37.
- Chen Q; W.Z. Zhou; G.H. Du and L.M. Peng (2002): Trititanate Nanotubes Made via a Single Alkali Treatment, *Adv. Mater.* 14: 1208.
- Zwilling V; M. Aucouturier and E. Darque-Certerti (1999): Anodic oxidation of titanium and TA6V alloy in chromic media. An electrochemical approach, *Electrochim. Acta* 45: 921.
- Ghicov A; H. Tsuchiya; J.M. Macak and P. Schmuki (2005): Titanium oxide nanotubes prepared in phosphate electrolytes, *Electrochem. Commun.* 7: 505.
- Shankar K; G.K. Mor; H.E. Prakasam; S. Yoriya; M. Paulose; O.K. Varghese and C.A. Grimes (2007): Highly-ordered TiO_2 nanotube arrays up to 220 μm in length: use in water photoelectrolysis and dye-sensitized solar cells, *Nanotechnology* 18: 065707.
- Gong D; C.A. Grimes; O.K. Varghese; W. Hu; R.S. Singh; Z. Chen and E.C. Dickey (2001): Titanium oxide nanotube arrays prepared by anodic oxidation, *J. Mater. Res.* 16: 3331.
- Prakasam H.E.; K. Shankar; M. Paulose; O.K. Varghese and C.A. Grimes (2007): A New Benchmark for TiO_2 Nanotube Array Growth by Anodization, *J. Phys. Chem. C* 111: 7241.
- Anitha V.C.; Deepthy Menon; Shantikumar V. Nair and R. Prasanth (2010): Electrochemical tuning of titania nanotube morphology in inhibitor electrolytes, *Electrochimica Acta* 55: 3703.
- Peng L; M.L. Eltgroth; T.J. LaTempa; C.A. Grimes and T.A. Desai (2009): The effect of TiO_2 nanotubes on endothelial function and smooth muscle proliferation, *Biomaterials* 30: 1268.

16. Brammer K.S; S. Oh; J.O. Gallagher and S. Jin (2008): Enhanced Cellular Mobility Guided by TiO₂ Nanotube Surfaces, *NanoLett*8: 786.
17. Oh S.H.; R.R. Finones; C. Daraio; L.H. Chen and S. Jin (2005): Growth of nano-scale hydroxyapatite using chemically treated titanium oxide nanotubes, *Biomaterials* 26: 4938.
18. Oh S.; K.S. Brammer; Y.S.J. Li; D. Teng; A.J. Engler and S. Chien (2009): Stem cell fate dictated solely by altered nanotube dimension, *PNAS* 106: 2130.
19. Park S. Bauer; K.A. Schlegel; F.W. Neukam J.; K. von der Mark and P. Schmuki (2009): TiO₂ Nanotube Surfaces: 15 nm—An Optimal Length Scale of Surface Topography for Cell Adhesion and Differentiation, *Small* 5: 666.
20. Kalbacova M; J.M. Macak; F. Schmidt-Stein; C.T. Mierke and P. Schmuki (2008): TiO₂ nanotubes: photocatalyst for cancer cell killing, *Phys Status Solid RRL* 2: 194.
21. Macak J.M; H. Tsuchiya; L. Taveira; S. Aldabergerova and P. Schmuki (2005): Smooth Anodic TiO₂ Nanotubes, *Angew. Chem. Int. Ed.* 44: 7463.
22. Albu S.P.; D. Kim and P. Schmuki (2008): Growth of aligned TiO₂ bamboo-type nanotubes and highly ordered nanolace, *Angew. Chem. Int. Ed.* 47: 1916.
23. Wang D.A; Y. Liu; B. Yu; F. Zhou and W.M. Liu (2009): TiO₂ Nanotubes with Tunable Morphology, Diameter, and Length: Synthesis and Photo-Electrical/Catalytic Performance, *Chem. Mater.* 21: 1198.
24. Han-Cheol Choe; Won-Gi Kim and Yong-Hoon Jeong (2010): Surface characteristics of HA coated Ti-30Ta-xZr and Ti-30Nb-xZr alloys after nanotube formation, *Surface and Coatings Technology* 205: S305.
25. Al-Mobarak N.A; A.A. Al-Swayih and F.A. Al-Rashoud (2011): Corrosion Behavior of Ti-6Al-7Nb Alloy in Biological Solution for Dentistry Applications, *Int. J. Electrochem. Sci.* 6: 2031.
26. Antony R.P; T. Mathews; S. Dash; A. K. Tyagi and B. Raj (2012): X-ray photoelectron spectroscopic studies of anodically synthesized self aligned TiO₂ nanotube arrays and the effect of electrochemical parameters on tube morphology , *Materials Chemistry and Physics* 132: 957.
27. Jaszay T; A. Caprani; F. Priem and J.P. Frayret (1988): On the anodic dissolution of titanium between 15°C and 100°C in deaerated 2 m hydrochloric acid, *Electrochimica Acta* 33: 1093.
28. Lohrengel M.M (1993): Thin anodic oxide layers on aluminium and other valve metals: high field regime, *Mater. Sci. Eng.* R11: 243.
29. Cabrera N. and N.F. Mott (1949): Theory of the oxidation of metals, *Rep. Prog. Phys.* 12: 163.
30. Schultze J.W and M.M. Lohrengel (2000): Stability, reactivity and breakdown of passive films. Problems of recent and future research, *Electrochim. Acta* 45: 2499.
31. Kong, D.S (2008): The Influence of Fluoride on the Physicochemical Properties of Anodic Oxide Films Formed on Titanium Surfaces, *Langmuir* 24: 5324.
32. Munoz A.G.; Q. Chen and P. Schmuki (2007): Interfacial properties of self-organized TiO₂ nanotubes studied by impedance spectroscopy , *J. Solid State, Electrochem.* 11: 1077.
33. Saji V. S.; H. C. Choe and W. A. Brantley (2009): An electrochemical study on self-ordered nanoporous and nanotubular oxide on Ti-35Nb-5Ta-7Zr alloy for biomedical applications, *Acta Biomaterialia* 5: 2303.
34. Hu T.; Y.C. Xin; S.L. Wu; C.L. Chu; J. Lu; L. Guan; H.M. Chen; T.F. Hung; K.W.K. Yeung and P.K. Chu (2011): Corrosion behavior on orthopedic NiTi alloy with nanocrystalline/amorphous surface, *Materials Chemistry and Physics* 126: 102.
35. Zhang Y.J.; C.W. Yan; F.H. Wang and W.F. Li (2005): Electrochemical behavior of anodized Mg alloy AZ91D in chloride containing aqueous solution, *Corros. Sci.* 47: 2816.
36. Yu W.Q.; J. Qiu; L. Xu and F.Q. Zhang (2009): Corrosion behaviors of TiO₂ nanotube layers on titanium in Hank's solution , *Biomed. Mater.* 4: 065012.
37. Saji V.S. and H.C. Choe (2009): Electrochemical corrosion behaviour of nanotubular Ti-13Nb-13Zr alloy in Ringer's solution, *Corros. Sci.* 51: 1658.
38. Chen X.; M. Schriver; T. Suen and S.S. Mao (2007): Fabrication of 10 nm diameter TiO₂ nanotube arrays by titanium anodization, *Thin Solid Films* 515; 8511.